

# UC Berkeley

## UC Berkeley Previously Published Works

### Title

A modular platform to develop peptoid-based selective fluorescent metal sensors.

### Permalink

<https://escholarship.org/uc/item/1wq154ct>

### Journal

Chemical communications (Cambridge, England), 53(24)

### ISSN

1359-7345

### Authors

Knight, Abigail S  
Kulkarni, Rishikesh U  
Zhou, Effie Y  
et al.

### Publication Date

2017-03-01

### DOI

10.1039/c7cc00931c

Peer reviewed



Published in final edited form as:

*Chem Commun (Camb)*. 2017 March 25; 53(24): 3477–3480. doi:10.1039/c7cc00931c.

## A modular platform to develop peptoid-based selective fluorescent metal sensors†

Abigail S. Knight<sup>‡,a</sup>, Rishikesh U. Kulkarni<sup>‡,a</sup>, Effie Y. Zhou<sup>a</sup>, Jenna M. Franke<sup>a</sup>, Evan W. Miller<sup>a,b,c</sup>, and Matthew B. Francis<sup>a,d</sup>

<sup>a</sup>Department of Chemistry, University of California, Berkeley, CA, 94720, USA

<sup>b</sup>Department of Molecular and Cell Biology, University of California, Berkeley, CA, 94720, USA

<sup>c</sup>Helen Wills Neuroscience Institute, University of California, Berkeley, CA, 94720, USA

<sup>d</sup>Materials Sciences Division, Lawrence Berkeley National Laboratories, Berkeley, CA, 94720, USA

### Abstract

Despite the reduction in industrial use of toxic heavy metals, there remain contaminated natural water sources across the world. Herein we present a modular platform for developing selective sensors for toxic metal ions using *N*-substituted glycine, or peptoid, oligomers coupled to a fluorophore. As a preliminary evaluation of this strategy, structures based on previously identified metal-binding peptoids were synthesized with terminal pyrene moieties. Both derivatives of this initial design demonstrated a turn-off response in the presence of various metal ions. A colorimetric screen was designed to identify a peptoid ligand that chelates Hg(II). Multiple ligands were identified that were able to deplete Hg(II) from a solution selectively in the presence of an excess of competing ions. The C-terminal fluoropeptoid derivatives demonstrated similar selectivity to their label-free counterparts. This strategy could be applied to develop sensors for many different metal ions of interest using a variety of fluorophores, leading to a panel of sensors for identifying various water source contaminants.

Several heavy metal pollutants exhibit immunotoxic and neurotoxic effects, resulting in damage to the central nervous system, endocrine system, and several organs in the body.<sup>1</sup> In particular, mercury contamination has drawn interest due to its bioaccumulation in the form of methylmercury and its dispersal throughout the environment as Hg(II) species.<sup>2</sup> These contaminants can be quantified with high accuracy in the laboratory using technologies such as inductively coupled plasma optical emission spectrometry (ICP-OES), but there is also a strong need for rapid, on-site detection tools based on inexpensive and operationally simple sensors.<sup>3</sup> Selectivity of such sensors is critical to choosing the appropriate remediation solution to detected contamination. To address this need, a number of fluorescent mercury sensors have been developed based on multidentate ionophores.<sup>4</sup> However, many of these

<sup>†</sup>Electronic supplementary information (ESI) available: Imaging parameters. Supporting figures and data. See DOI: 10.1039/c7cc00931c

Correspondence to: Evan W. Miller; Matthew B. Francis.

<sup>‡</sup>These authors contributed equally.

systems require difficult syntheses or exhibit incompatibilities with high ionic strength water samples. In addition, mercury sensors often respond to similar ions, such as lead(II) and copper(II), limiting accuracy in complex samples.<sup>5</sup>

A major challenge of developing new fluorescent sensors is the design of chelators possessing both high affinity and high selectivity, as both are required for the accurate detection of a contaminant in unprocessed environmental samples. Heavy metal pollutants are normally present in water at concentrations several orders of magnitude lower than innocuous ions ( $\text{Na}^+$ ,  $\text{Mg}^{2+}$ ,  $\text{Ca}^{2+}$ , *etc.*). While numerous fluorescent metal sensors exist, even well-known chelators such as the calcium-binding BAPTA group demonstrate significant affinity for other divalent cations.<sup>6</sup> It is difficult to address this lack of selectivity using rational design alone.

As a complementary approach, combinatorial methods have been demonstrated for the rapid identification of selective ligands for metals.<sup>7</sup> Peptoids, or *N*-substituted glycine oligomers, have demonstrated significant promise in this field due to their compatibility with combinatorial synthesis and assay techniques, large set of side chain functional groups, and low cost.<sup>8</sup> In general, thousands of ligand candidates are prepared using efficient synthetic techniques. The resulting library is then screened for the binding of a metal ion of interest using colorimetric<sup>7b</sup> or spectroscopic<sup>7c</sup> detection methods. When large excesses of competing ions are added to these screens, a subset of ligands can be identified that retain the ability to bind the target ion. A variety of peptoid-based ligands have been reported,<sup>9</sup> and previously described uses of this combinatorial strategy have found new peptoid ligands capable of binding  $\text{Cr}(\text{VI})$ ,<sup>7b</sup>  $\text{Cd}(\text{II})$ ,<sup>7d</sup> and uranyl<sup>7e</sup> in complex media. Taking advantage of well established interactions of metal ions with fluorescent ligands,<sup>10</sup> herein we establish an efficient platform for the development of selective fluorescent sensors by combining selective peptoid ligands prepared simply on solid supports with an inexpensive non-coordinating fluorophore, pyrene.

The ligand first chosen to investigate design strategies was a previously reported peptoid-based  $\text{Cr}(\text{VI})$  ligand that demonstrated selectivity for chromium in the presence of an excess innocuous ions commonly found in water.<sup>7b</sup> Two different pyrene derivatives, 1-pyrenebutyric acid and 1-pyrenemethylamine, were incorporated at the C- and N-termini of the peptoid,<sup>11</sup> respectively (**1**, Fig. 1a, and **2**, ESI,† Fig. S1). Following synthesis of **1** and **2** and purification *via* RP-HPLC, the impact of metal coordination on the fluorescence was evaluated with a panel of eleven metals assayed at concentrations ranging from 1  $\mu\text{M}$  to 90  $\mu\text{M}$  in a buffered solution (100 mM HEPES, pH 7.4, 1 mM NaCl, 1 mM  $\text{MgSO}_4$ ). A summary of the normalized fluorescence data for **1** is shown in Fig. 1b, and complete titration spectra and binding curves for **1** and **2** are shown in Fig. S1 (ESI†). For most metal ions, a change in fluorescence was observed upon metal coordination (decreasing from 1.0 to the value shown in Fig. 1b). This decrease can be attributed to an energy transfer process that results in quenching of the fluorophore, resulting in an “off-state” in the presence of metal. The N-terminal fluoropeptoid, **2**, showed a 10-fold lower quantum yield compared to **1** due to quenching from the N-terminal amine. This can be decreased by that amine binding to metals, leading to competing effects.

To develop a sensor that could identify the presence of a single contaminant, we designed a new screen to identify Hg(II)-binding peptoid ligands with selectivity over Cr(VI), Pb(II), and Cd(II) based on our previous work<sup>5</sup> (Fig. 2a). This library contained four variable positions, one position containing one of three potential “turn” moieties (Fig. 2a), and a photolabile moiety. Three aminohexanoic linker residues were also incorporated first on the PEG-grafted polystyrene resin to create cleavable, high-mass structures facilitating sequence identification with MALDI-TOF-TOF MS/MS. Sequence diversity was generated *via* split-and-pool synthesis, resulting in a library of 7203 members.

To identify ligands that bind Hg(II) selectively, a screening medium that contained an excess of Cr(VI), Cd(II), Pb(II), and innocuous ions found in high concentrations in water was desired. Due to the insolubility of lead chromate, the screen was completed in a new screening procedure with two sequential steps (Fig. 2b). The first used an excess of Cr(VI) and Cd(II) (2.5mM each) with Hg (250  $\mu$ M) in bis(TRIS) buffer (pH 7, 50 mM), plus Na(I), Mg(II), and Ca(II) (2.5 mM each). The second screen used a similar buffer, but with Pb(II) instead of Cr(VI) (Fig. 2b). A sample of resin from the library was pre-swelled in water and then incubated in the screening medium for 1–4 h before isolation *via* vacuum filtration and a brief water rinse. In order to visualize the beads, a solution of diphenylcarbazide was applied. In the presence of Cr(VI), diphenylcarbazide forms a pink complex, while in the presence of Hg(II), it forms a deep purple complex (Fig. S2a, ESI<sup>†</sup>). The dye was applied in ethanol, which was then evaporated to leave the dye trapped in the beads (Fig. S2, ESI<sup>†</sup>). The purple beads were identified using a light microscope, selected, and the bound dye and ions were removed using a previously described protocol.<sup>7b</sup> These selected beads were screened again in the lead-containing medium. The dye and metal ions were again removed from the beads. Photocleavage followed by MS/MS sequencing resulted in the identification of seven unique mercury binding peptoids (Fig. S3, ESI<sup>†</sup>).

Identified structures contained a single Nle residue with varying numbers of Nbu and Npip residues. While thiols are common ligands (*i.e.* Nthe) for heavy metals, it is likely thiol-containing ligands were not selected due to affinity for the competing ions (*e.g.*, Cd(II) or Pb(II)). Previous work has identified imidazoles as having selective affinity for mercury.<sup>12</sup> Therefore, we hypothesized that the hydrophobic residues contributed to forming a binding pocket of the correct size and electrostatic environment. To probe differences in affinity and selectivity among the seven structures, they were resynthesized on the PEG-grafted resin and exposed to solutions with mercury (10-fold excess) and an excess of other ions (100-fold or larger excess). After a 2 h incubation, an aliquot was removed and diluted for characterization with ICP-OES to determine the concentrations of mercury, chromium, cadmium, and lead (Fig. 3 and Fig. S4, ESI<sup>†</sup>). Mercury sequence 6, or “Hg-peptoid”, successfully depleted Hg(II) from the samples while having negligible effect on the concentrations of the Pb(II), Cd(II), and Cr(VI) in the solutions.

Hg-peptoid was converted to N- and C-terminal fluoro-peptoids using the same protocols described above, resulting in C-fluoro-peptoid **3** (Fig. 4a) and N-fluoro-peptoid **4** (Fig. S5, ESI<sup>†</sup>). Following purification with RP-HPLC, the Hg-fluoro-peptoids were screened against the same panel of eleven metals. A sample titration of **3** with Hg(II) can be seen in Fig. 4b ( $K_d = 120 \pm 50 \mu$ M, assuming 1 : 1 complexation) and a summary of the normalized data

can be seen in Fig. 4c. N-Fluoropeptoid **4** shows very little response to any of the eleven metals screened. However, C-fluoropeptoid **3** demonstrated a substantial decrease in fluorescence in the presence of mercury while showing little, if any, response to most metals and a small turn-off response to Fe(II), Co(II), and Cu(II). Furthermore, **3** retained its ability to detect mercury even in the presence of these other metals (Fig. S5, ESI†). C-Fluoropeptoid **3** demonstrated a 64% loss in fluorescence at 90  $\mu\text{M}$  Hg(II) and a 45% loss in fluorescence at 35  $\mu\text{M}$  Hg(II), a concentration relevant for mercury pollution.<sup>9e</sup>

We were encouraged that converting Hg-peptoid into a C-terminal fluoropeptoid appeared to have little effect on the selectivity profile of its binding, while replacing a hydrophobic residue (Npip) resulted in a loss of selectivity (Fig. S5, ESI†), supporting the hypothesis that the selected structure forms a binding “pocket” in which all of the residues play an essential role. To confirm the correlation of binding with changes in fluorescence, a control structure (**5**) was synthesized without a coordinating imidazole and demonstrated no decrease in fluorescence in the presence of relevant ions (Fig. S6, ESI†).

Due to the intrinsic brightness of pyrene, we then chose to assess C-fluoropeptoid **3** as a simple sensor for mercury in contaminated water samples. In order to simulate mercury pollution, water samples were obtained from Ocean Beach in San Francisco, CA and Strawberry Creek in Berkeley, CA to represent ocean and stream water, respectively. Solutions of C-fluoropeptoid **3** in these water samples were prepared and titrated with mercury (Fig. 5a). The observed decrease in fluorescence was significantly less in ocean water and significantly more in stream water when compared to the experimental buffer. The fluorescence of pyrene has a high dependence on environmental factors, including ionic strength, so calibration in comparable media would be recommended.

As a quantifiable method for “on-site” detection, samples of C-fluoropeptoid **3** (10  $\mu\text{M}$ ) and Hg(II) (0, 35, 75, and 150  $\mu\text{M}$ ) were prepared in stream water and placed into a transparent 96 well tray. The tray was then imaged using a Gel Doc EZ system using UV excitation and imaging in the Oriole channel (Fig. 5b and c). C-fluoropeptoid **3** showed a large decrease in fluorescence in the presence of mercury that recapitulated the data gathered using fluorimetry. Due to its intrinsic brightness, selectivity, and water solubility, C-fluoropeptoid **3** could be used as a visible sensor for on-site quantification of mercury in water samples with simple tools, such as a handheld UV light.

In summary, we present a new platform for the development of selective fluorescent metal sensors based on a modular peptoid scaffold. We identified a selective ligand for mercury(II) and combined it with a fluorophore to produce a selective fluorescent sensor for Hg(II) that retains the scalability and operational simplicity of the peptoid scaffold. The mercury sensor developed is bright and selective, offering potential for the fabrication of an on-site tool for the detection of Hg(II) in environmental water samples. The discovery platform can easily be implemented for other metal ions or quenchable fluorophores, potentially affording sensors for many different metal targets with a variety of fluorescence properties.

## Supplementary Material

Refer to Web version on PubMed Central for supplementary material.

## Acknowledgments

This work was supported by the UC Berkeley Hellman Fellows Fund, NIH (R00NS078561 and R35GM119855, EWM), and the NSF (CHE-1413666, MBF). ASK was supported by a Philomathia Fellowship in Environmental Sciences. ASK, RUK and JMF were supported by a training grant from the NIH (T32GM066698). EYZ was supported by the Berkeley Chemistry Department.

## References

1. (a) Stacchiotti A, Morandini F, Bettoni F, Schena I, Lavazza A, Grigolato PG, Apostoli P, Rezzani R, Aleo MF. *Toxicology*. 2009; 264:215–224. [PubMed: 19720107] (b) Clarkson TW, Magos L, Myers GJ. *N. Engl. J. Med.* 2003; 349:1731–1737. [PubMed: 14585942]
2. Blum JD, Popp BN, Drazen JC, Choy CA, Johnson MW. *Nat. Geosci.* 2013; 6:879–884.
3. Li M, Gou H, Al-Ogaidi I, Wu N. *ACS Sustainable Chem. Eng.* 2013; 1:713–723.
4. (a) Yoon S, Albers AE, Wong AP, Chang CJ. *J. Am. Chem. Soc.* 2005; 127:16030–16031. [PubMed: 16287282] (b) Nolan EM, Lippard SJ. *J. Am. Chem. Soc.* 2007; 129:5910–5918. [PubMed: 17429971] (c) Yoon S, Miller EW, He Q, Do PH, Chang CJ. *Angew. Chem., Int. Ed.* 2007; 46:6658–6661. (d) Domaille DW, Que EL, Chang CJ. *Nat. Chem. Biol.* 2008; 4:168–175. [PubMed: 18277978] (e) Voutsadaki S, Tsikalas GK, Klontzas E, Froudakis GE, Katerinopoulos HE. *Chem. Commun.* 2010; 46:3292–3294.
5. (a) Lin W-C, Wu C-Y, Liu Z-H, Lin C-Y, Yen Y-P. *Talanta*. 2010; 81:1209–1215. [PubMed: 20441886] (b) Prathish KP, James D, Jaisy J, Rao TP. *Anal. Chim. Acta.* 2009; 647:84–89. [PubMed: 19576390] (c) Lee MH, Kang G, Kim JW, Ham S, Kim JS. *Supramol. Chem.* 2009; 21:135–141. (d) Wang M, Yan F, Zou Y, Chen L, Yang N, Zhou X. *Sens. Actuators, B.* 2014; 192:512–521. (e) Tang L, Li F, Liu M, Nandhakumar R. *Spectrochim. Acta, Part A.* 2011; 78:1168–1172.
6. Tsien RY. *Biochemistry*. 1980; 19:2396–2404. [PubMed: 6770893]
7. (a) Martin LJ, Sculimbrene BR, Nitz M, Imperiali B. *QSAR Comb. Sci.* 2005; 24:1149–1157. (b) Knight AS, Zhou EY, Pelton JG, Francis MB. *J. Am. Chem. Soc.* 2013; 135:17488–17493. [PubMed: 24195610] (c) Nalband DM, Warner BP, Zahler NH, Kirshenbaum K. *Biopolymers.* 2014; 102:407–415. [PubMed: 25059748] (d) Knight AS, Zhou EY, Francis MB. *Chem. Sci.* 2015; 6:4042–4048. (e) Parker BF, Knight AS, Vukovic S, Arnold J, Francis MB. *Ind. Eng. Chem. Res.* 2016; 55:4187–4194.
8. (a) Simon RJ, Kania RS, Zuckermann RN, Huebner VD, Jewell DA, Banville S, Ng S, Wang L, Rosenberg S, Marlowe CK. *Proc. Natl. Acad. Sci. U. S. A.* 1992; 89:9367–9371. [PubMed: 1409642] (b) Knight AS, Zhou EY, Francis MB, Zuckermann RN. *Adv. Mater.* 2015; 27:5665–5691. [PubMed: 25855478]
9. (a) Lee B-C, Chu TK, Dill KA, Zuckermann RN. *J. Am. Chem. Soc.* 2008; 130:8847–8855. [PubMed: 18597438] (b) Maayan G, Ward MD, Kirshenbaum K. *Chem. Commun.* 2009:56–58. (c) Maayan G. *Eur. J. Org. Chem.* 2009:5699–5710. (d) Zabrodski T, Baskin M, Kaniraj PJ, Maayan G. *Synlett.* 2015:461–466. (e) Baskin M, Maayan G. *Biopolymers.* 2015; 104:577–584. [PubMed: 25969151] (f) Baskin M, Maayan G. *Chem. Sci.* 2016; 7:2809–2820. [PubMed: 28660058] (g) Prathap KJ, Maayan G. *Chem. Commun.* 2015; 51:11096–11099.
10. Frabrizzi L, Licchelli M, Pallavicini P, Perotti A, Taglietti A, Sacchi D. *Chem. – Eur. J.* 1996; 2:75–82.
11. Burkoth TS, Fafarman AT, Charych DH, Connolly MD, Zuckermann RN. *J. Am. Chem. Soc.* 2003; 125:8841–8845. [PubMed: 12862480]
12. (a) Brooks P, Davidson N. *J. Am. Chem. Soc.* 1960; 82:2118–2123. (b) Onyido I, Norris AR, Buncel E. *Chem. Rev.* 2004; 104:5911–5930. [PubMed: 15584692] (c) Wang X-F, Lv Y, Okamura T, Kawaguchi H, Wu G, Sun W-Y, Ueyama N. *Cryst. Growth Des.* 2007; 6:1125–1133.

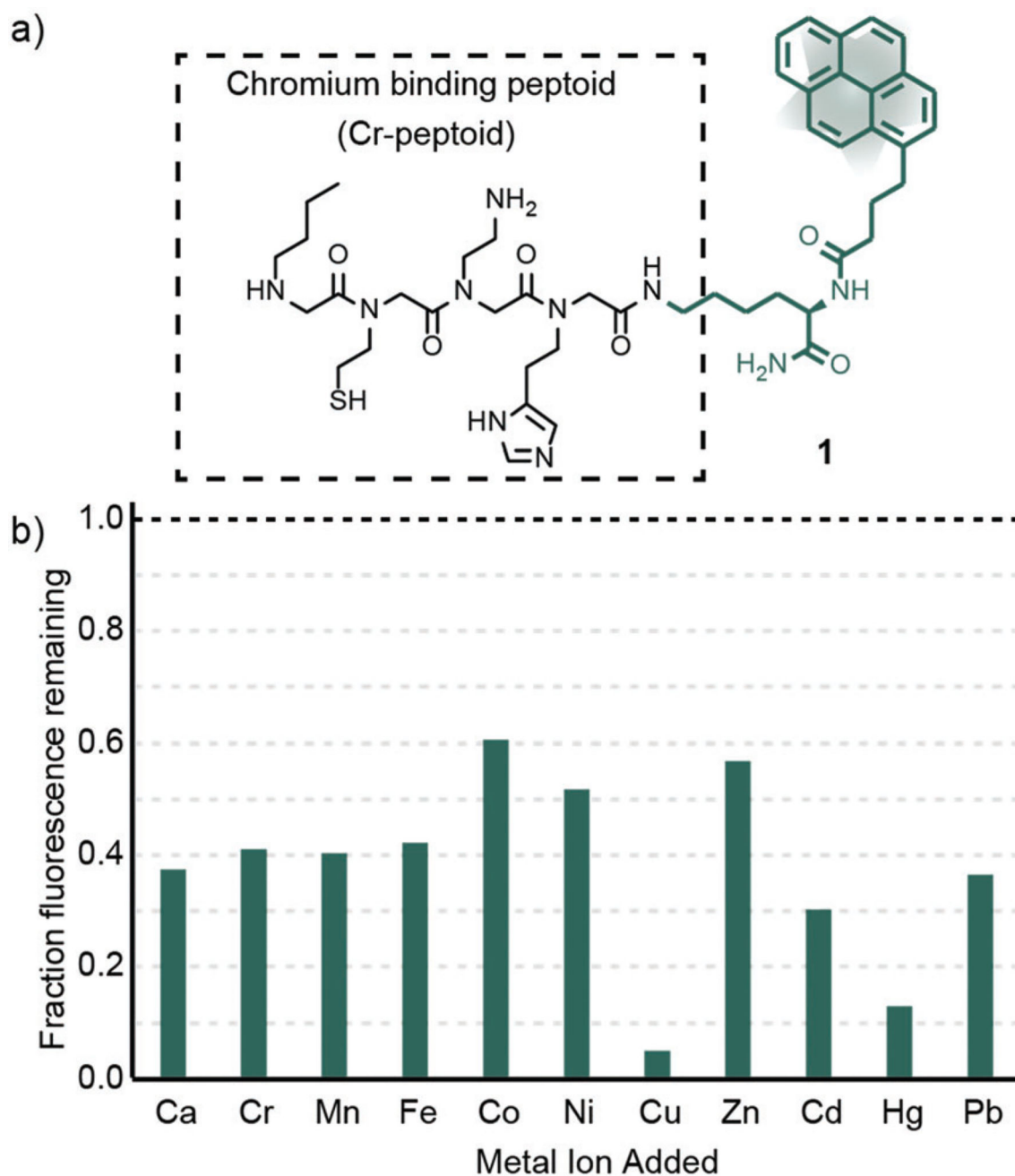


**Fig. 1.** Design and evaluation of chromium binding fluoro-peptoid. (a) Schematic illustrating the synthesis of the C-fluoro-peptoid by attaching a modifiable lysine residue to the C-terminus of the peptoid. (b) Evaluation of the fluorescence of **1** after the addition of metal ions (90  $\mu\text{M}$ ) in a buffered solution (HEPES, 100 mM, pH 7, plus 1 mM NaCl). Each bar represents the ratio of peptoid fluorescence in the presence of the metal ion to that in its absence.



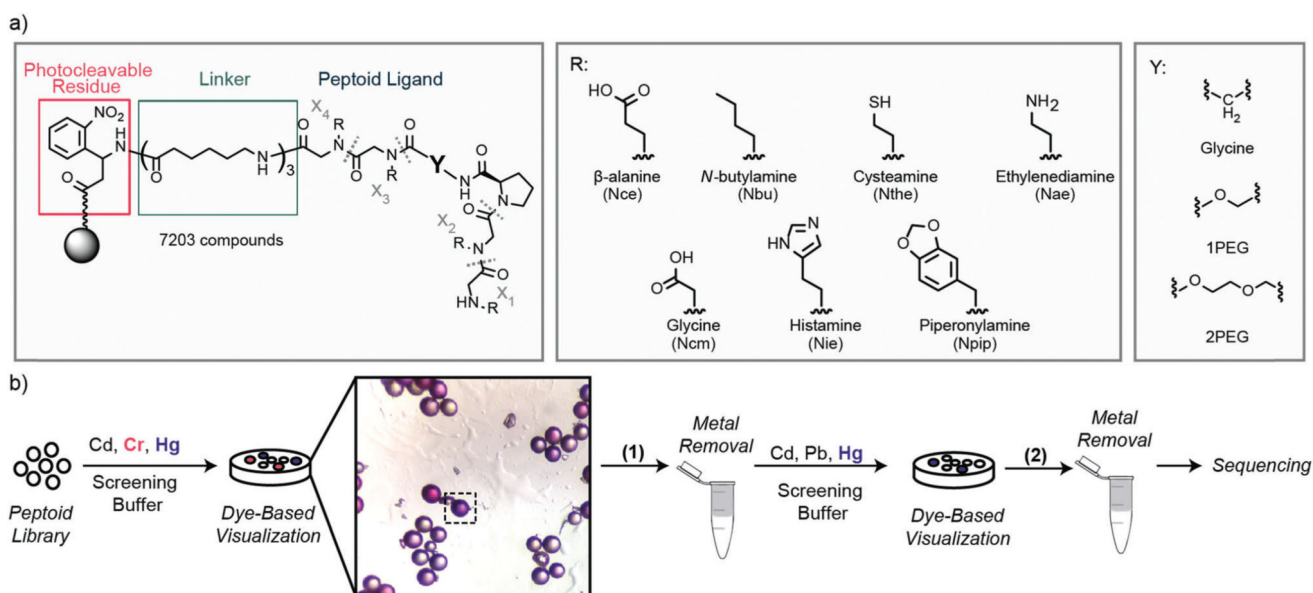


**Fig. 2.**

Combinatorial screen to identify a selective mercury ligand. (a) Schematic of the peptoid library. Each peptoid contains four variable residues ( $X_n$ ) connected by a turn in the middle of the structure. (b) Due to the low solubility of lead chromate, the screen for mercury affinity had to be completed in two steps. During the first step (1) a screen was completed in the presence of 2.5 mM  $\text{Cr}^{6+}$ , 2.5 mM  $\text{Cd}^{2+}$ , and 250  $\mu\text{M}$   $\text{Hg}^{2+}$  in a screening buffer (50 mM bis(TRIS), pH 7, plus 25 mM  $\text{Na}^+$ , and 25 mM  $\text{Mg}^{2+}$ , and 2.5 mM  $\text{Ca}^{2+}$ ). The bound metal ions were visualized with a solution of diphenylcarbazide. A photograph of the first step in the screening process is shown with a purple bead (indicating bound mercury) highlighted. Then the ions were removed from the identified sequences and the screen was repeated (2) with  $\text{Pb}^{2+}$  instead of  $\text{Cr}^{6+}$ .



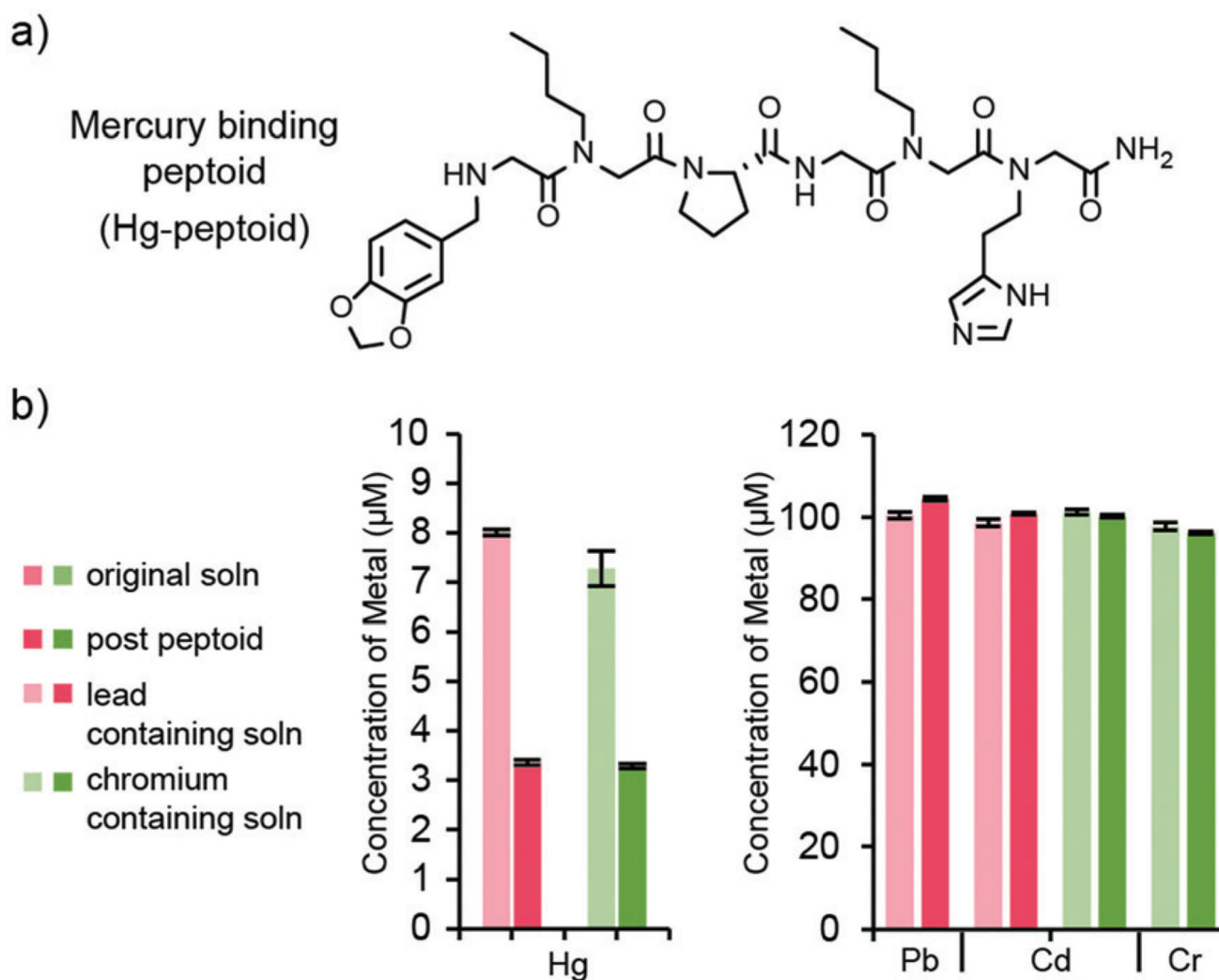


**Fig. 3.** Selective mercury binding peptoid. (a) Structure of one of the identified sequences. (b) An evaluation of the ability of the Hg-peptoid to deplete  $\text{Hg}^{2+}$  ( $8 \mu\text{M}$ ) in a significant excess of additional toxic metals ( $100 \mu\text{M}$ ) and ions commonly in high concentrations in water ( $\text{Na}^+$ ,  $\text{Mg}^{2+} - 25\text{mM}$  and  $\text{Ca}^{2+} - 2.5 \text{mM}$ ). Error bars represent the standard error with  $n = 3$ .

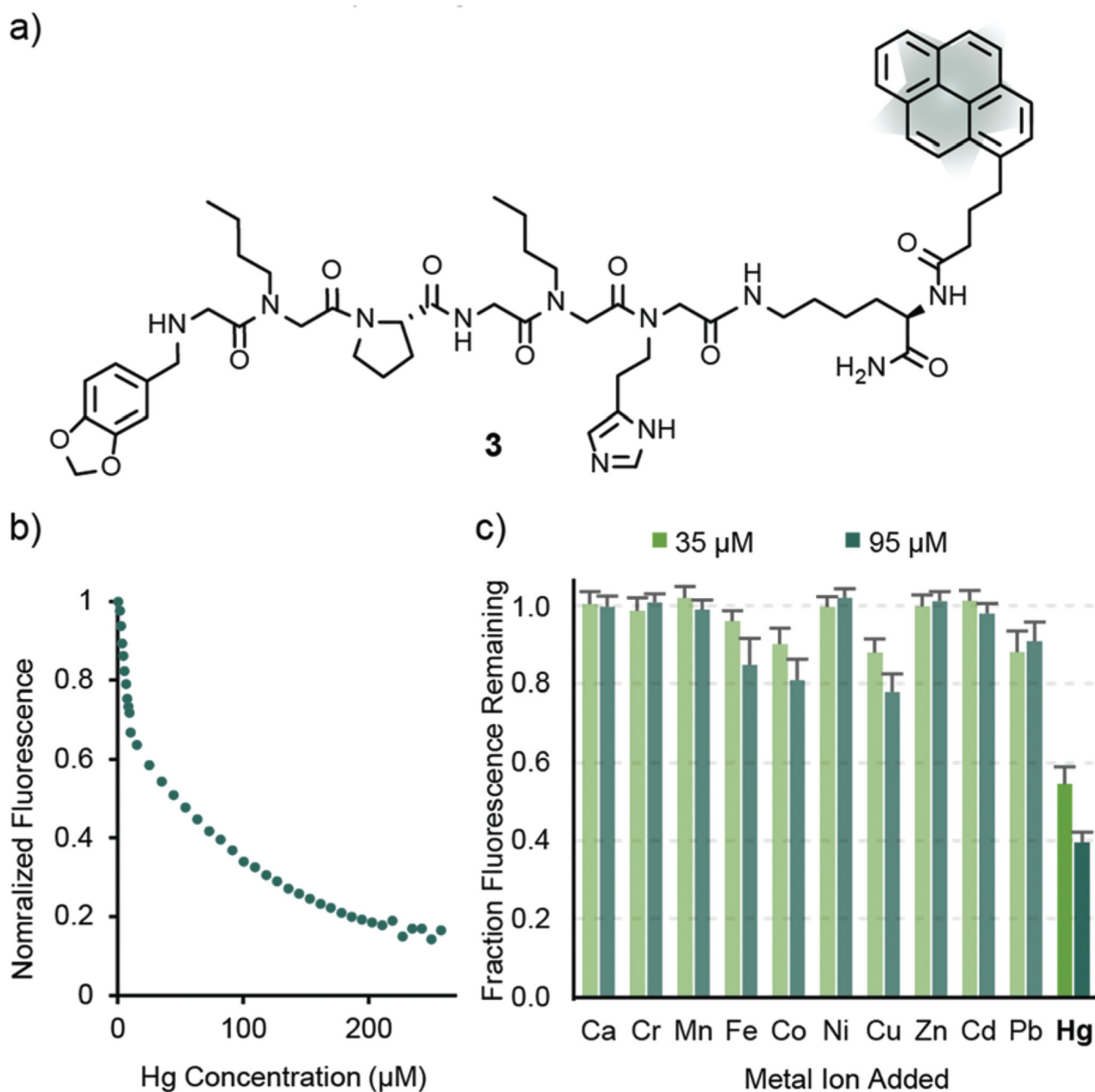


**Fig. 4.** Affinity and selectivity of mercury fluoropeptoid **3**. (a) Structure of C-fluoropeptoid **3**. (b) Fluorescence turn-off of **3** (1  $\mu\text{M}$  in HBS buffer) in the presence of 1 to 315  $\mu\text{M}$  of  $\text{Hg}^{2+}$ . (c) The fluorescence signal of **3** in the presence of 35  $\mu\text{M}$  or 90  $\mu\text{M}$  of the indicated ions in HBS. The values are normalized to the fluorescence of **3** in the same buffer with 90  $\mu\text{M}$   $\text{Na}^+$ , and the error bars represent the standard error of  $n = 3$  samples.

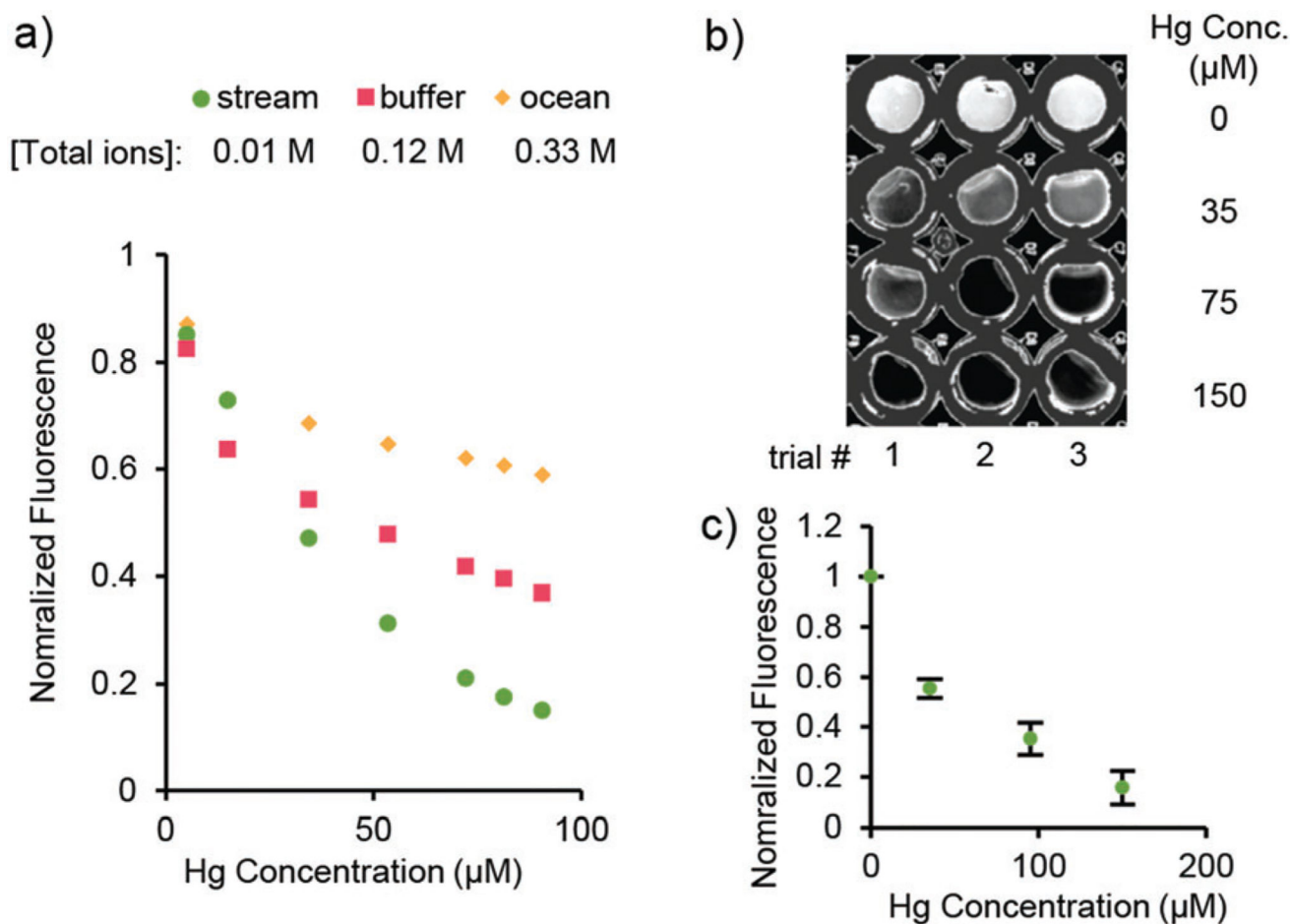


Fig. 5.

Fluorescence of **3** in natural water sources. (a) The fluorescence of **3** in stream water, HBS, and ocean water in the presence of various concentrations of  $\text{Hg}^{2+}$ . (b) A Gel Doc image of **3** (10  $\mu\text{M}$ ) in stream water with four concentrations of mercury. (c) A quantification of the image in (b). The error bars represent the standard error with  $n = 3$  samples.